

Validating a Predictive Structure–Property Relationship by Discovery of Novel Polymers which Reduce Bacterial Biofilm Formation

Adam A. Dundas, Olutoba Sanni, Jean-Frédéric Dubern, Georgios Dimitrakis, Andrew L. Hook, Derek J. Irvine, Paul Williams, and Morgan R. Alexander*

Synthetic materials are an everyday component of modern healthcare yet often fail routinely as a consequence of medical-device-centered infections. The incidence rate for catheter-associated urinary tract infections is between 3% and 7% for each day of use, which means that infection is inevitable when resident for sufficient time. The O'Neill Review on antimicrobial resistance estimates that, left unchecked, ten million people will die annually from drug-resistant infections by 2050. Development of biomaterials resistant to bacterial colonization can play an important role in reducing device-associated infections. However, rational design of new biomaterials is hindered by the lack of quantitative structure–activity relationships (QSARs). Here, the development of a predictive QSAR is reported for bacterial biofilm formation on a range of polymers, using calculated molecular descriptors of monomer units to discover and exemplify novel, biofilm-resistant (meth)acrylate-based polymers. These predictions are validated successfully by the synthesis of new monomers which are polymerized to create coatings found to be resistant to biofilm formation by six different bacterial pathogens: *Pseudomonas aeruginosa*, *Proteus mirabilis*, *Enterococcus faecalis*, *Klebsiella pneumoniae*, *Escherichia coli*, and *Staphylococcus aureus*.

The concept of the post-antibiotic era is becoming a reality, with patients presenting with infections from bacterial pathogens that resist multiple last line antibiotics while at the same time, very few novel antimicrobial drugs are coming onto the market.^[1–5] As multi-antibiotic resistance becomes widespread,^[6] the prevention of bacterial infections has become an urgent healthcare priority in order to reduce morbidity and mortality.^[7–9] Medical-device-related infections are a consequence of planktonic bacteria attaching to the surface of implanted devices and developing into surface-associated “slime” layers called biofilms, which have been reported to be 1000 times more resistant to antibiotic and host immune system clearance.^[10–13]

High throughput materials discovery screens have been utilized to discover polymers that reduce bacterial surface colonization in order to circumvent our poor understanding of material surface-bacteria interactions that leaves us ill-equipped to design new materials from first principles.^[14]


Novel coatings were identified by screening a commercially available (meth)acrylate monomer library for polymers that successfully reduced biofilm formation by *P. aeruginosa*, *S. aureus*, and *E. coli* in laboratory cultures in vitro and in vivo in a foreign body mouse infection model.^[15,16] Such screening experiments facilitate the rapid assessment of readily available monomers to identify hit materials for a particular application, such as reducing bacterial fouling of surfaces in industry and healthcare, the expansion of pluripotent stem cells, increasing the maturation of cardiomyocyte derived from stem cells, and providing bioinstructive implant materials.^[16–19]

To maximize the productivity of materials discovery screening campaigns, the monomer building blocks should ideally be cheap, easy to process, and readily accessible, i.e., not requiring time consuming bespoke synthesis. Acrylate/acrylamide monomers that are commercially available with wide chemical diversity (hundreds of different compounds) are suitable for this as they are readily printable and amenable to in situ polymerization.^[20,21] To synthesize variants of these materials in-house, we have used a single step, transesterification synthesis (see scheme Figure S1a in the Supporting Information) that utilizes

Dr. A. A. Dundas, O. Sanni, Dr. A. L. Hook, Prof. M. R. Alexander
Advanced Medical and Healthcare Technologies
School of Pharmacy
University of Nottingham
Nottingham NG7 2RD, UK
E-mail: Morgan.Alexander@nottingham.ac.uk

Dr. A. A. Dundas, Dr. G. Dimitrakis, Prof. D. J. Irvine
Department of Chemical and Environmental Engineering
Faculty of Engineering
University of Nottingham
Nottingham NG7 2RD, UK

Dr. J.-F. Dubern, Prof. P. Williams
Centre of Biomolecular Sciences
School of Life Sciences University of Nottingham
Nottingham NG7 2RD, UK

 The ORCID identification number(s) for the author(s) of this article can be found under <https://doi.org/10.1002/adma.201903513>.

© 2019 The Authors. Published by WILEY-VCH Verlag GmbH & Co. KGaA, Weinheim. This is an open access article under the terms of the Creative Commons Attribution License, which permits use, distribution and reproduction in any medium, provided the original work is properly cited.

DOI: 10.1002/adma.201903513

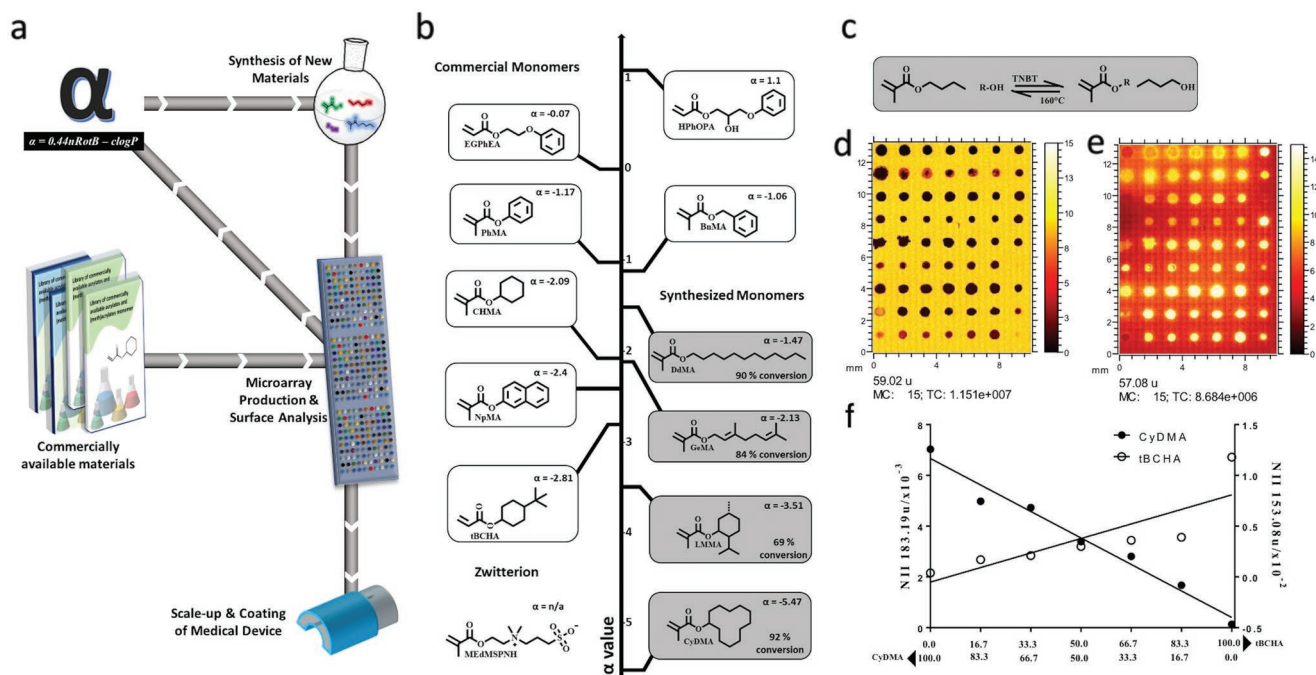


Figure 1. a) Process for developing and validating a predictive model at the microscale level including testing on a medical device. Hundreds of commercially available materials are assessed for their ability to reduce bacterial biofilm formation via high throughput screening. Processed data is used to identify a “hit” material and scaled-up to coat medical devices for confirmatory in vitro studies. Analyzed data together with material properties are used to generate models that predict new untested materials which are synthesized and reincorporated into the materials library for further screening. This repeated cycle refines the theoretical model and makes it a more powerful predictor of “hit” performance. b) Materials library made up of 12 monomers positioned along the α value vertical axis. c) Reaction scheme for the transesterification synthesis reaction at 160 °C with titanium butoxide (TNBT) catalyst. d, e) ToF SIMS ion images from one replicate area of the microarray corresponding to $C_2H_3O_2^-$ (m/z 59.02) (d) and $C_4H_9^+$ (m/z 57.07) (e), both displayed from 0 to 15 normalized counts. f) Graphs of normalized ion intensity (NII) for representative SIMS ions for copolymers of tBCHA with CyDMA. The content (%) of each monomer is indicated below graph. The representative ion for tBCHA is $C_{10}H_{17}O^-$ indicative of tBCHA ($R^2 = 0.68$) and $C_{12}H_{23}O^-$ indicative of CyDMA ($R^2 = 0.97$).

commercially available alcohols (thousands are readily available) to create bespoke monomer building blocks that significantly expand the chemical space relative to the commercial (meth)acrylates used to date. Typical polymer microarray approaches use unbiased screening of as wide a range of materials or “chemical space” as possible to maximize the chances of identifying hit materials that surpass the performance of existing material solutions. To date, this process has been very successful in identifying a class of monomers that surpass conventional silicone catheters for preventing catheter-associated urinary tract infections, resulting in the granting of a CE mark for a urinary catheter device.^[16,19,22] To guide synthesis beyond the commercially available compounds computational modeling has been used to generate structure–function relationships that can predict the biological performance of virtual materials.^[23–25] In the case of bacterial biofilm formation a simple parameter combining the partition coefficient ($\log P$) and the number of rotatable bonds for hydrocarbon acrylate pendant groups pointed towards a route to a more targeted approach for materials discovery, although until now this has not been experimentally validated (Figure 1a).^[26] Here, we validate a modification of that QSAR by extrapolating from the correlation identified between the bacterial biofilm formation and a monomer molecular descriptor parameter, α , to predict novel biofilm resistant monomers which were not included in the initial library.

α comprises the log of the calculated partition coefficient ($\log P$) and the number of rotatable bonds ($nRotB$), $\alpha = 0.44nRotB - \log P$ for each monomer previously developed from a polymer microarray library.^[26] Using this as a starting point, a polymer of the novel monomer cyclododecyl methacrylate (CyDMA) was predicted to offer improved prevention of biofilm formation by virtue of its low (-5.47) α value. Here we confirm this prediction both using polymer microarray screening experiments and subsequent multigram synthesis of both monomer and polymer. The α parameter was also shown to be valid for a range of other bespoke materials synthesized with values outside of the previously accessed range using commercially available monomers (of -2.81 to 1.10). Upon scale-up, pCyDMA produced an average 55-fold reduction in individual surface coverage for all six bacterial pathogens compared with silicone catheters, and 14-fold compared to silver hydrogel coated catheters, and fourfold reduction in biofilm formation for the six pathogens compared to a previously identified hit polymer coating (poly(ethylene glycol dicyclopentyl ether acrylate-co-diethyleneglycol methacrylate p(EGDPEA-co-DEGMA)).

The molecular structures of several monomers with low α parameter values were identified for synthesis, shown in Figure 1b, to expand the chemical space in order to identify improved materials. This also tested the validity of correlation between bacterial

biofilm formation and the α parameter beyond the initial library limited to commercially available compounds. An α value of -5.47 was calculated for CyDMA and -3.51 for 5-methyl-2-(1-methylethyl) cyclohexyl methacrylate (LMMA), which is lower than all materials previously tested ($\alpha = -3$ to 1).^[26]

Four monomers were successfully synthesized using the one-step transesterification route (Figure S1a, Supporting Information), (CyDMA, *trans*-3,7-dimethyl-2,6-octadienyl methacrylate (GeMA), LMMA, dodecyl methacrylate (DdMA)) outlined in Figure 1b, with conversions of 92%, 82%, 69%, and 92%, respectively (see Figures S1–S5 in the Supporting Information for NMR spectroscopy studies). In addition to the four synthesized monomers, eight commercially available monomers that had been previously tested were also included for comparison. A polymer microarray was printed using 11 monomers with an α value range of -5.47 to 1.1 mixed pairwise with *tert*-butyl cyclohexyl acrylate (tBCHA) to produce unique polymer spots printed in triplicate on a single slide after photo polymerization with an α value range of -5.47 to 1.1 (Figure 1b). Time-of-flight secondary ion mass spectrometry (ToF-SIMS) was employed to monitor spot printing fidelity and provide surface analysis to detect any surface segregation due to demixing of monomers (Figure 1d–f).^[27] Unique ions were identified for most monomers and used to monitor the relationship between monomer feed ratio and the surface composition of the polymer product. The ion intensities indicate linear trends for the SIMS ion intensity versus composition when mixing the two monomers, cyclododecyl methacrylate (CyDMA) and *tert*-butyl cyclohexyl acrylate (tBCHA) (Figure 1f) with correlation coefficients of $R^2 = 0.97$ and $R^2 = 0.68$ respectively. In both cases the pure monomers exhibit slightly higher intensity than predicted by a straight-line fit to all the data, suggesting possible matrix effect nonlinearity. All the copolymer series were found to approximate to the bulk ratios apart from 6-octadienyl methacrylate (GeMA) and ethylene glycol phenyl ether acrylate (EGPhEA) where surface segregation when mixed with *tert*-butyl cyclohexyl acrylate was inferred (Figure S8, Supporting Information). This is likely due to differences in the miscibility of the monomers causing phase separation before polymerization is complete—copolymers which exhibited this were not studied further herein.^[28]

To determine whether unreacted reagents (monomers and their associated alcohols) could inhibit bacterial growth and hence reduced bacterial attachment and biofilm formation, *P. aeruginosa* was cultured over 24 h in RPMI media dosed with monomers and the associated alcohols at concentrations of 0.01%–0.1% (v/v) (Figures S9 and S10, Supporting Information). Further bacterial growth studies were conducted on the catalysts and the scaled-up monomers for all six pathogens (Figures S11 and S12, Supporting Information). No bacteriostatic or bactericidal effects were observed, with the exception of LMMA which caused a 50% reduction in growth compared with the untreated control. Therefore, materials containing LMMA were omitted from the subsequent polymer microarray analysis. It is also possible that esterase enzymes produced by bacteria could cleave and release pendant alcohol groups that contribute to the lack of biofilm formation on resistant materials. To investigate whether this was a factor, degradation of benzyl methacrylate polymer sample was quantified after treatment with fast-acting porcine liver esterase (PLE) over 2 h; no

degradation was observed for the polymers, in contrast to the monomers which were readily cleaved (Figures S13–S16, Supporting Information). It is likely that the increased steric hindrance and/or the electronic stability of the ester moiety in poly(acrylates) prevented cleavage of the polymer side chains. These results suggest that the biofilm inhibition observed on all polymers (excepting LMMA) was not influenced by soluble compounds released from the materials, but instead by the response of the bacterial to the polymer surface.

The human pathogenic bacteria *P. aeruginosa*, *Pr. mirabilis*, and *S. aureus* were chosen for initial biofilm formation experiments with polymer microarrays, shown in Figure 2, as they include both gram-positive (*S. aureus*) and gram-negative (*P. aeruginosa*, *Pr. mirabilis*) bacterial species, and are frequently associated with healthcare-associated infections including catheter-associated urinary tract infections (CAUTI).^[29]

A linear correlation ($R^2 = 0.77$) was observed between the bacterial load measured as fluorescence intensity of *P. aeruginosa* versus α between -3 and 1.1 (Figure 2c).^[26] However, when materials in the extended range of α of -5.47 to 1.1 were considered, a poorer linear correlation ($R^2 = 0.61$) was observed. As α decreased, bacterial fluorescence approached a lower limit under these microarray assay conditions. An exponential fit better described the relationship between α and *P. aeruginosa* attachment for the full polymer library dataset ($R^2 = 0.79$) (Figure 2c). While weaker correlation was observed for *Pr. mirabilis* ($R^2 = 0.52$) (Figure 2d), these correlations suggest that both species respond to the physicochemical properties described by the α value (hydrophilicity and molecular rigidity). Attachment of *S. aureus*, a nonmotile gram-positive bacterial species, showed no correlation with α suggesting that other factors are dominant (Figure S17, Supporting Information). As the lowest α parameter materials were statistically similar for both bacterial species, the CyDMA homopolymer was taken forward for further investigation as a coating on silicone catheter segments in order to carry out initial comparison with the biofouling performance of existing devices.

Polymerization of CyDMA was undertaken using thermal polymerization to produce a polymer solution with which to dip-coat silicone catheter segments. For comparison using the same scale-up test, a high performing acrylate copolymer material previously reported in the literature to prevent bacterial biofilm formation, poly(ethylene glycol dicyclopentyl ether acrylate-co-diethyleneglycol methacrylate p(EGDPEA-co-DEGMA), was similarly polymerized and coated onto silicone catheter segments.^[16] An example of a high α value polymer, neopentyl glycol propoxylate diacrylate (NGPDA) was polymerized using the same route and coated onto catheter sections: NGPDA has an α value of 2.96 compared to CyDMA ($\alpha = -5.47$). Uncoated silicone catheter and silver hydrogel coated catheters were commercially sourced and used as comparators that are applied in clinical practice. To mimic environmental conditions associated with CAUTI, bacteria were cultured in artificial urine (AU) with the five different surfaces to quantify both single and mixed species bacterial biofilm formation with 6 clinically relevant bacterial species: *P. aeruginosa*, *Pr. mirabilis*, *E. faecalis*, *K. pneumoniae*, *E. coli*, and *S. aureus* (Figure 3).

On silicone catheter segments a mean bacterial biomass (averaging all six strains) of $25 \pm 2.9 \mu\text{m}^3/\mu\text{m}^2$ was observed

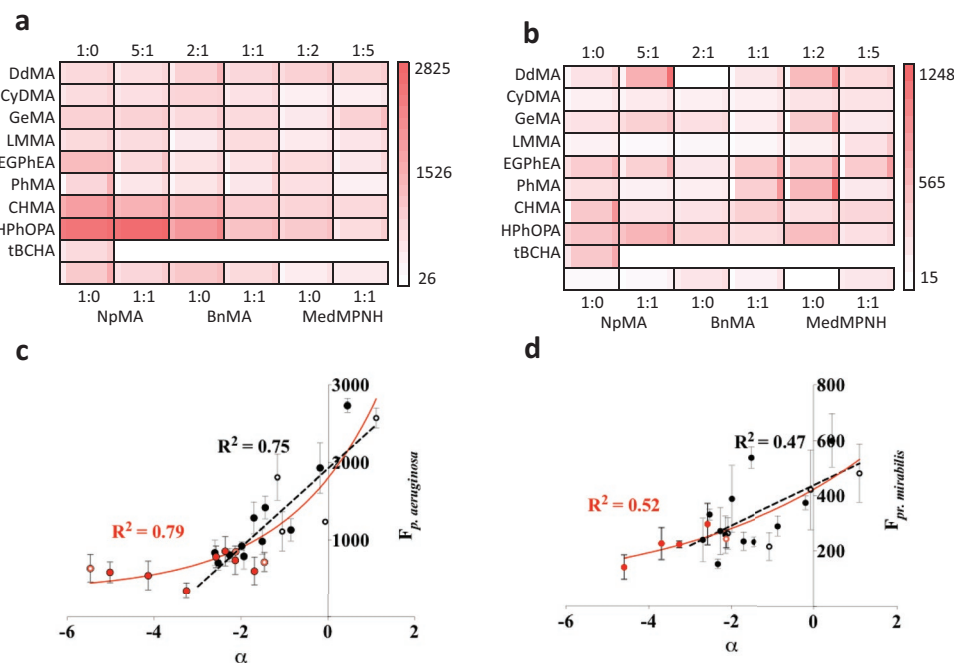


Figure 2. a) Results from polymer microarray biological assay with mCherry tagged *P. aeruginosa*. Monomer identity is organized into rows and mixing ratio columns with *tert*-Butyl cyclohexyl acrylate (tBCHA). The center square is the fluorescence value for attachment of *P. aeruginosa* (red indicating high bacterial adhesion and white low bacterial adhesion), whilst the narrow columns to the left or right indicate ± 1 sd unit respectively ($N = 3$). b) Results from the same experiment as inset (a) but with dsRed tagged *Pr. mirabilis* ($n = 3$). c) Fluorescence intensity measured from *P. aeruginosa* attachment to the polymer microarray. The unfilled/solid black symbols represent materials used to build the α model (homopolymers/copolymers respectively), the dashed black line is the linear relationship from -3 to 1.1 , $R^2 = 0.75$. The red unfilled/solid symbols are materials used to extend α range (homopolymers/copolymers respectively) and red solid line is exponential relationship with values from -5.47 to 1.1 , $R^2 = 0.79$, error bars shown are ± 1 sd ($n = 3$). d) Fluorescence from *Pr. mirabilis* attachment to the polymer library using the same display conventions as for (c).

compared with the reduced load of $6.4 \pm 2.2 \mu\text{m}^3/\mu\text{m}^2$ on a commercial silver hydrogel coated catheter (Figure 3a). In contrast, the pCyDMA coated catheter segment successfully prevented biofilm formation by all six individual bacterial species with a mean biomass of only $0.5 \pm 0.2 \mu\text{m}^3/\mu\text{m}^2$ as shown in Figure 3a,b. The p(EGDPEA-co-DEGMA)^[16] coating also performed well, with a mean biomass of $1.6 \pm 0.4 \mu\text{m}^3/\mu\text{m}^2$, although this was surpassed in performance by the pCyDMA discovered in this QSAR process. The high α value polymer, pNGPDA, performance was consistent with the microarray relationships identified, with an average biomass of $21.9 \pm 3.4 \mu\text{m}^3/\mu\text{m}^2$, showing an approximate 44-fold greater biomass compared with pCyDMA.

Most CAUTI infections are polymicrobial.^[30] To test the biofilm resistance of a dual species biofilm, we used GFP-labeled *S. aureus* SH1000 (green) and mCherry labeled *P. aeruginosa* (red) inoculated onto the catheter segments in a 10:1 ratio. Figure 3c–e shows that for silicone, pCyDMA, and p(EGDPEA-co-DEGMA) after 72 h incubation, the dual species biofilm completely covered the silicone surface, whereas very little biofilm coverage was observed on p(EGDPEA-co-DEGMA) and was almost completely absent on pCyDMA and the quantification of this mixed biofilm can be found in Figure S18 in the Supporting Information.

In summary, we have used a QSAR model (α) to successfully predict bacterial biofilm formation on a new polymer (pCyDMA) which we synthesized along with others using

a polymer microarray. Coating of catheter segments with pCyDMA reduced biofilm formation by six commonly associated urinary tract pathogens by 32–300 fold (average 55 fold) compared with an uncoated silicone catheter and 9–85 fold (average 14 fold) compared with a commercial silver hydrogel coated catheter. This polymer coating outperformed our previously identified best polymer (pEGDPEA) determined by experimental screening using a high throughput discovery approach with an average fourfold improvement. Furthermore, pCyDMA was also shown to prevent the formation of dual-species biofilm in artificial urine, exemplifying the uses of the material in a more realistic medical-device-associated infection scenario. This illustrates how validated QSAR models with simple physical molecular descriptions can be used to predict novel materials that improve on previously established materials that have great potential to reduce medical-device-associated infections.

Experimental Section

Materials: All materials were used as supplied without further purification unless otherwise stated in the preparations detailed below.

Transesterification Experiments: In a typical reaction butyl methacrylate (Sigma-Aldrich) (14 g, 98.5 mmol) was introduced into a 50 mL vessel along with the required quantity of individual target alcohols [cyclododecanol (VWR) (13 g, 70.5 mmol), trans-3,7-dimethyl-2,6-octadien-1-ol (10.8 g, 70.3 mmol) 5-methyl-2-(1-methylethyl)

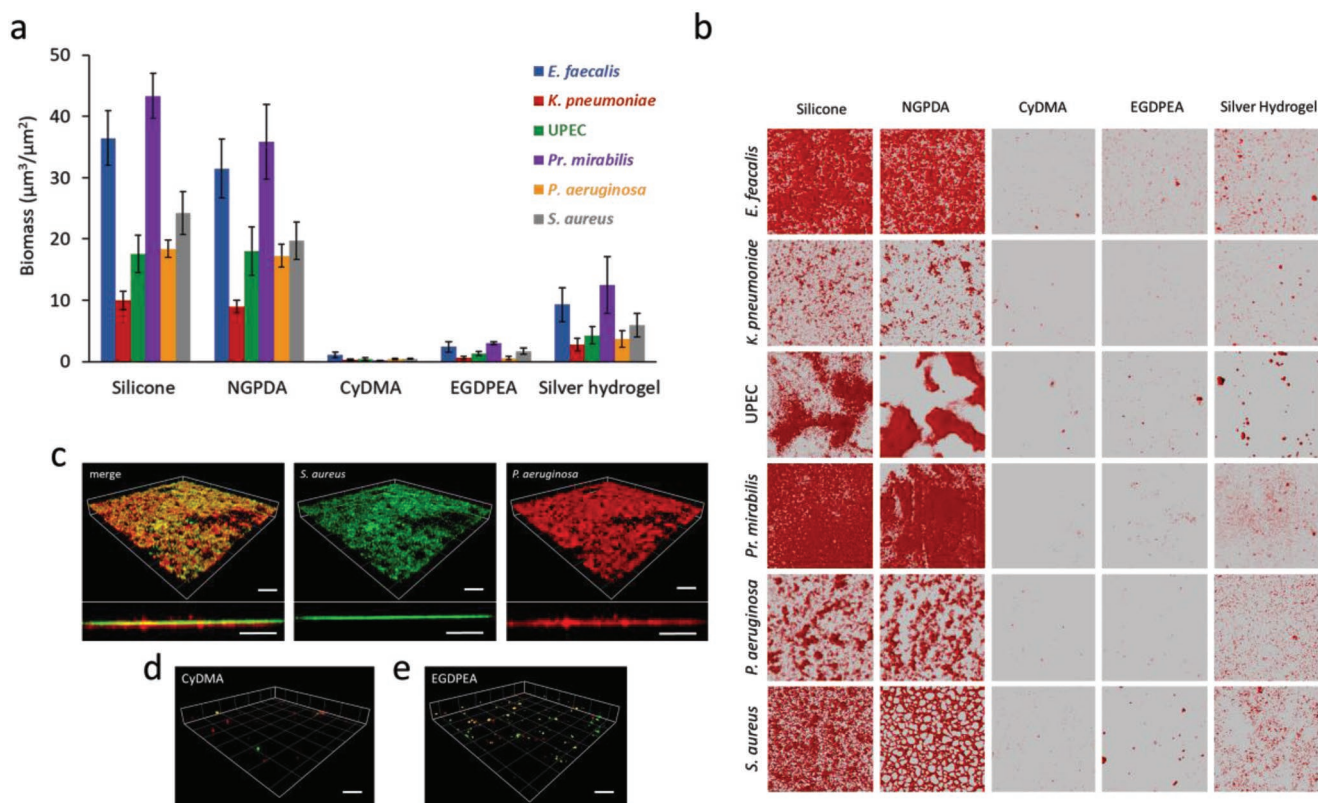


Figure 3. a) Surface coverage by single species (*E. faecalis*, *K. pneumoniae*, *E. coli*, *Pr. mirabilis*, *P. aeruginosa*, and *S. aureus*) biofilms quantified after 72 h incubation on silicone, silver hydrogel, pNGPDA, pCyDMA, and p(EGDPEA-co-DEGMA) (labeled EGDPEA) coated silicone catheter segments in AU. Error bars equal ± 1 sd unit, $n = 3$. b) The corresponding confocal microscopy images for Syto64 stained *E. faecalis*, *K. pneumoniae*, *E. coli*, *Pr. mirabilis*, *P. aeruginosa*, and *S. aureus* growing on each polymer surface. Each image is $160 \times 160 \mu\text{m}$. c) 3D representation and transverse view of a dual-species biofilm formed on glass: GFP-tagged *S. aureus* SH1000 (green) and mCherry labeled *P. aeruginosa* (red) in a 10:1 ratio. d–e) Three dimensional representation and transverse view showing the lack of mature biofilm on pCyDMA and pEGDPEA. Scale bars represent $50 \mu\text{m}$.

cyclohexanol (11.2 g, 71.6 mmol) or 1-dodecanol (Sigma-Aldrich) (13.1 g, 70.3 mmol)] to form a 7:5 molar ratio. Then titanium butoxide (Sigma-Aldrich) catalyst at a concentration of 1% by molar ratio (relative to butyl methacrylate) and 1000 ppm of 4-methoxyphenol (Sigma-Aldrich) inhibitor were added. The reaction was heated to 160°C and stirred for 45 min at which point a nitrogen gas sparge was introduced to increase the rate of removal of butanol by-product. Butyl methacrylate has been chosen as the methacrylate precursor for these reactions to allow these elevated temperatures to drive the reaction kinetics and equilibrium toward full completion in a short timescale. The reaction was sampled every 15 min and these samples were quenched in a freezer prior to NMR analysis.

Bacterial Strains and Growth Conditions: *Pr. mirabilis* strain Hauser 1885, *P. aeruginosa* strain PAO1 (Washington sub-line, Nottingham collection), *S. aureus* SH1000, *E. faecalis* NCTC12697, *K. pneumoniae* NCIMP10104, and uropathogenic *Escherichia coli* (UPEC) were routinely grown at 37°C in lysogeny broth (LB) with shaking at 200 rpm or on LB agar (2% w/v). Where required, plasmids for constitutively expressing fluorescent proteins GFP (pBK-miniTn7-egfp) and mCherry (pMMR) were introduced into the relevant host strain by conjugation or electroporation.

Supporting Information

Supporting Information is available from the Wiley Online Library or from the author.

Acknowledgements

A.A.D. and O.S. contributed equally to this work. M.R.A., D.J.I., and P.W. are the joint senior authors. The authors would like to kindly acknowledge Emma Daffern and Samara Dawson for their assistance in the production of polymer microarrays. This work was supported by the Engineering and Physical Sciences Research Council [Grant no. EP/N006615/1] and the Wellcome Trust [Grant nos. 103882 and 103884]. The University of Nottingham is kindly acknowledged for funding A.L.H.'s Nottingham Research Fellowship. All relevant data are available from the University of Nottingham's Research Data Management Repository.

Conflict of Interest

The authors declare no conflict of interest.

Keywords

biofilms, low-fouling, polymer microarrays, quantitative structure–activity relationships, transesterification

Received: June 3, 2019

Revised: August 26, 2019

Published online:

- [1] M. Tyers, G. D. Wright, *Nat. Rev. Microbiol.* **2019**, *17*, 141.
- [2] J. Y. H. Lee, I. R. Monk, A. Gonçalves da Silva, T. Seemann, K. Y. L. Chua, A. Kearns, R. Hill, N. Woodford, M. D. Bartels, B. Strommenger, F. Laurent, M. Dodémont, A. Deplano, R. Patel, A. R. Larsen, T. M. Korman, T. P. Stinear, B. P. Howden, *Nat. Microbiol.* **2018**, *3*, 1175.
- [3] M. J. Renwick, D. M. Brogan, E. Mossialos, *J. Antibiot.* **2016**, *69*, 73.
- [4] A. J. Alanis, *Arch. Med. Res.* **2005**, *36*, 697.
- [5] E. K. Schneider, F. Reyes-Ortega, T. Velkov, J. Li, *Essays Biochem.* **2017**, *61*, 115.
- [6] D. Torumkuney, N. Mayanskiy, M. Edelstein, S. Sidorenko, R. Kozhevnikov, I. Morrissey, *J. Antimicrob. Chemother.* **2018**, *73*, 14.
- [7] S. L. Percival, L. Suleman, C. Vuotto, G. Donelli, *J. Med. Microbiol.* **2015**, *64*, 323.
- [8] L. E. Nicolle, *Antimicrob. Resist. Infect. Control* **2014**, *3*, 23.
- [9] J. O'Neill, *Comm. by UK Gov.* **2016**.
- [10] J. W. Costerton, P. S. Stewart, E. P. Greenberg, *Science* **1999**, *284*, 1318.
- [11] R. Bayston, L. E. Fisher, K. Weber, *Biomaterials* **2009**, *30*, 3167.
- [12] R. M. Donlan, *Emerg. Infect. Dis.* **2001**, *7*, 277.
- [13] C. W. Hall, T. Mah, *FEMS Microbiol. Rev.* **2017**, *41*, 276.
- [14] J. Kohn, T. Road, *Nat. Mater.* **2004**, *3*, 745.
- [15] A. L. Hook, C.-Y. Chang, J. Yang, J. Lockett, A. Cockayne, S. Atkinson, Y. Mei, R. Bayston, D. J. Irvine, R. Langer, D. G. Anderson, P. Williams, M. C. Davies, M. R. Alexander, *Nat. Biotechnol.* **2012**, *30*, 868.
- [16] A. L. Hook, C.-Y. Chang, J. Yang, S. Atkinson, R. Langer, D. G. Anderson, M. C. Davies, P. Williams, M. R. Alexander, *Adv. Mater.* **2013**, *25*, 2542.
- [17] A. K. Patel, M. W. Tibbitt, A. D. Celiz, M. C. Davies, R. Langer, C. Denning, M. R. Alexander, D. G. Anderson, *Curr. Opin. Solid State Mater. Sci.* **2016**, *20*, 202.
- [18] G. Tourniaire, J. Collins, S. Campbell, H. Mizomoto, S. Ogawa, J.-F. Thaburet, M. Bradley, *Chem. Commun.* **2006**, *20*, 2118.
- [19] A. D. Celiz, J. G. W. Smith, A. K. Patel, A. L. Hook, D. Rajamohan, V. T. George, L. Flatt, M. J. Patel, V. C. Epa, T. Singh, R. Langer, D. G. Anderson, N. D. Allen, D. C. Hay, D. A. Winkler, D. A. Barrett, M. C. Davies, L. E. Young, C. Denning, M. R. Alexander, *Adv. Mater.* **2015**, *27*, 4006.
- [20] A. D. Celiz, J. G. W. Smith, A. K. Patel, R. Langer, D. G. Anderson, D. A. Barrett, L. E. Young, M. C. Davies, C. Denning, M. R. Alexander, *Biomater. Sci.* **2014**, *2*, 1604.
- [21] D. G. Anderson, S. Levenberg, R. Langer, *Nat. Biotechnol.* **2004**, *22*, 863.
- [22] Y. Mei, K. Saha, S. R. Bogatyrev, J. Yang, A. L. Hook, Z. I. Kalcioğlu, S.-W. Cho, M. Mitalipova, N. Pyzocha, F. Rojas, K. J. Van Vliet, M. C. Davies, M. R. Alexander, R. Langer, R. Jaenisch, D. G. Anderson, *Nat. Mater.* **2010**, *9*, 768.
- [23] V. C. Epa, A. L. Hook, C. Chang, J. Yang, R. Langer, D. G. Anderson, P. Williams, M. C. Davies, M. R. Alexander, D. A. Winkler, *Adv. Funct. Mater.* **2014**, *24*, 2085.
- [24] A. S. Vasilevich, A. Carlier, J. De Boer, S. Singh, *Trends Biotechnol.* **2017**, *35*, 743.
- [25] S. Lin, S. Ryu, O. Tokareva, G. Gronau, M. M. Jacobsen, W. Huang, D. J. Rizzo, D. Li, C. Staii, N. M. Pugno, J. Y. Wong, D. L. Kaplan, M. J. Buehler, *Nat. Commun.* **2015**, *6*, 6892.
- [26] O. Sanni, C.-Y. Chang, D. G. Anderson, R. Langer, M. C. Davies, P. W. Williams, P. Williams, M. R. Alexander, A. L. Hook, *Adv. Healthcare Mater.* **2014**, *4*, 695.
- [27] A. L. Hook, D. J. Scurr, J. C. Burley, R. Langer, D. G. Anderson, M. C. Davies, M. R. Alexander, *J. Mater. Chem. B* **2013**, *1*, 1035.
- [28] A. L. Hook, J. Yang, X. Chen, C. J. Roberts, Y. Mei, D. G. Anderson, R. Langer, M. R. Alexander, M. C. Davies, *Soft Matter* **2011**, *7*, 7194.
- [29] R. M. Donlan, J. W. Costerton, *Clin. Microbiol. Rev.* **2002**, *15*, 167.
- [30] U. Römling, C. Balsalobre, *J. Intern. Med.* **2012**, *272*, 541.